

Geology and Geochemical Studies of Metatexite And Diatexite Migmatites From Bauchi, Northeastern Nigeria

Muhammad Nafisatu Magaji*¹, Ahmad Isah Haruna¹, Abdulmajid Isa Jibrin¹, Oshelike Ishioma Bridget¹

¹Department of Applied Geology, AbubakarTafawaBalewa University, Bauchi, Nigeria.

Received Date: 30 May 2021

Revised Date: 02 July 2021

Accepted Date: 11 July 2021

Abstract - The study addressed the geochemical properties of rocks of the study area. In this study, the geological mapping was done on a scale of 1:25,000 through an orderly method of mapping along with profiles from one outcrop to another by noting road and river channel that reveals subsurface lithology to understand the geology of the area. Samples of fresh representative rocks units were taken at each location with a corresponding coordinate. A total of 20 samples were collected, sorted, and grouped using Sawyer's (2008) first- and second-order morphological classifications of migmatites into four on the basis of morphology, and ten (10) representative rock samples were picked for whole-rock geochemical analysis (XRF). The results obtained show that the area has four distinct lithologic units. Viz, metatexite, melanocratic diatexite, mesocratic diatexite and leucocratic diatexite of different morphologic classes. The range of silica for metatexites and diatexites are 54.3wt.% to 65wt.% and 79.7wt.% to 86.0wt.% respectively. Both the metatexites and the diatexites shows overlapping compositions and the decreasing/ increasing trends on harker diagrams indicates that both are petrogenetically related. However, from the plot of frost tectonic discrimination the rock groups occupy both the ferroan and magnesian fields and relating it further to alumina saturation index, the peraluminous property of the diatexites implies high development of k-feldspar with continuous fractional crystallization, as the system is cooling and temperature is dropping in forming the leucocratic diatexitest

I. INTRODUCTION

The study area falls within Bauchi sheet 149 N.E within the northeastern Nigerian Basement Complex with coordinates of latitudes N10°21'00" & N10°23'00" and longitudes 09°50'00" E & 09°55'00"E (figure.1). The area of study is characterized generally by low to medium level outcrops and covers a total landmass of about 42 square kilometers with an average elevation of 590 meters above sea level. The area is fairly accessible through untarred roads, footpaths and cattle tracks with a network of stream channels. This present work

is aimed at understanding the geology and geochemical properties of rocks within the study area with emphasis on the morphological forms.

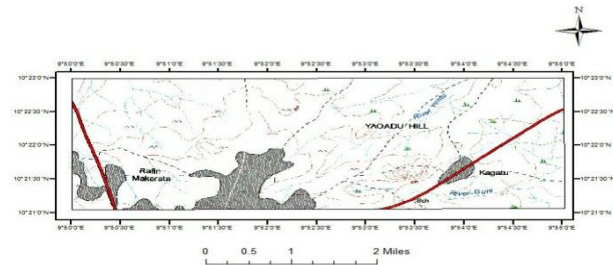


Figure 1: Location map of the study area drawn from Arcmap 10.1

II. Literature Review

The study area falls within the Neoproterozoic Trans-Saharan Belt and the Migmatization has been dated to 500±100Ma (Ferre, 2006). It was suggested to be formed from the converging West African Craton, the Congo Craton and East Saharan Block which was probably a Craton until 700Ma (Black and Liegeois, 1993) when it was widely and largely reactivated, except in few areas. Its rocks are mainly metamorphic consisting of monotonous granite-high-grade gneisses and migmatites cut by large Pan-African monzogranite plutons. Also, the close relationships between the regional tectono-metamorphic evolution of gneisses, regional anatexis and emplacement of syn-kinematic plutons from the monzodioritecharnockite association within the study area strongly suggest that the area underwent a monocyclic metamorphic history (Ferre et al, 1998). Moreover, migmatites are high-grade rocks that have been formed by partial melting, developed in various tectonic settings and can affect a wide range of protoliths. Consequently, rock packages are commonly chemically inhomogeneous at a variety of scale, so also the process of migmatization is correspondingly inhomogeneous throughout



a rock package and across a metamorphic complex. This inhomogeneity is particularly evident within rock types of the study area. Thus, their appearances and arrangements results in very complex morphologies that varies considerably from place to place within the study area. In conclusion, several geologists such as, Ferre et al. (1998), Ferre and Caby (2006), Oyawoye (1962) & (1964) have discoursed on the geology of this region and the results of their studies declared a single stage of metamorphic evolution. The geology of the study area is distinguished by rocks of high-grade granulite facies metamorphic assemblages, principally metatexites, melanocratic diatexite, mesocratic diatexite and leucocratic diatexite (figure. 2).

III. MATERIAL AND METHODS

The method of mapping along profiles from one outcrop to another through logging of river channel and road that reveals subsurface lithology was adopted in the field during the course of this work to understand the geology of the area. Samples of fresh representative rocks units were taken at each location with a corresponding coordinate. A total of 20 samples were collected, sorted and grouped using Sawyer’s (2008) first- and second-order morphological classifications of migmatites into four on the basis of morphology from which 10 representative samples were picked for X-ray fluorescence spectrometer at the Nigerian Geological Survey Agency, Kaduna state, Nigeria. The geochemical results of major oxides (wt%) and minor/trace elements (ppm) (table 1) below was used to generate the various geochemical plots whereas rock classification system of Cross, Iddings, Pirsson and Washington (CIPW) and granite mesonorms were computed to ascertained index/accessory minerals (table 2).

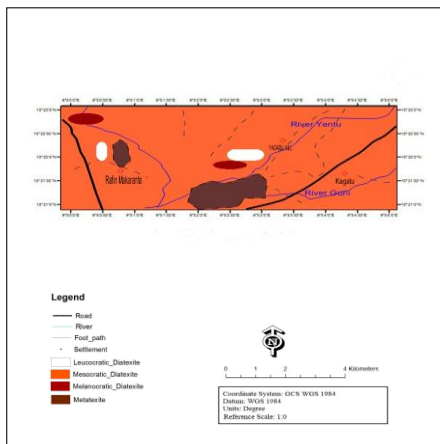


Figure 2: Geologic map of the study area from Surfer 13 and ArcMap 10.1

IV. Results

A. Field relation and morphology of the rock groups

Migmatitic assemblages can be grouped in to metatexites and diatexites on the basis of their field appearances (Sawyer 1987). The Metatexite is migmatite that preserves coherent, pre-partial melting structures in the palaeosome and residuum, whereas diatexite has disaggregated and lost structural coherency. Morphologically, stromatic metatexite migmatite (figure 3A) is distinguished by numerous, thin parallel and laterally persistent leucosomes having pre-partial melting structures that is primary layering in the protolith preserved. Melanocratic diatexite (figure 3B) predominantly ranges from leucocratic portion (quartz and feldspar) to melanocratic portion (ferromagnesian minerals). The neosome is variable in appearance, it includes leucosome and melanosome in varying proportions. Morphologically, the mesocratic diatexite of the study area has pre-migmatization structures which include bedding and foliation destroyed while within the neosome, a lighter coloured portion consisting of quartz and feldspar is sandwiched between darker colored parts rich in ferromagnesian minerals (figure 3C). Homogenization and coarsening of texture is true of leucocratic diatexite of the study area (figure 3D), the rock material is coarsely grained with an igneous texture having small volume of ferromagnesian minerals and a high k-feldspar and plagioclase ratio.



Figure 3: (A) field occurrence of stromatic metatexite migmatite, (B) field occurrence of melanocratic diatexite migmatite, (C) field view of mesocratic diatexite migmatite, (D) field view of leucocratic diatexite migmatite within the area of study.

B. Geochemical computation

Whole-rock geochemical examination have been determined on the representative rock groups of the study area. Major and trace elements results of these groups is given below (table 1).

a) Harker Variation Diagram

Variation diagram (figure 4) has concentration of oxides plotted on the vertical axis against silica on the horizontal axis. The range of silica for metatexites and diatexites are

54.3wt.% to 65wt.% and 79.7wt.% to 6.0wt.% respectively. As concentrations of (CaO, MgO, TiO₂, Al₂O₃, and FeO) increases, the concentration of SiO₂ also increases. While concentrations of K₂O and Na₂O decreases with increase in SiO₂ concentration. In general, the plots show good trends of

decreasing CaO, MgO, TiO₂, Al₂O₃, and FeO, with increasing SiO₂ from metatexites to leucocratic diatexites and increasing K₂O and Na₂O with decreasing SiO₂ from leucocratic diatexites to metatexites.

Table 1: Geochemical Data Table

Sampl es	1	2	3	4	5	6	7	8	9	10
SiO ₂	54.3	58.5	61.2	65.5	79.7	79.5	80.9	82.2	80	86
CaO	4.24	6.02	7.4	4.08	1.5	1.6	0.6	0.61	0.84	0.54
MgO	4	4.4	8.06	3	0.6	0.5	0.23	0.32	0.02	0.06
SO ₃	0.13	0.12	ND	0.04	ND	ND	0.014	0.012	0.026	ND
K ₂ O	1	0.48	ND	0.58	1.3	1.2	1.2	3.8	4	1
Na ₂ O	0.3	0.2	ND	0.43	0.42	0.43	0.8	1.23	1.04	1.02
TiO ₂	2.01	1.87	1.12	1.3	0.95	1.1	0.68	0.22	0.18	0.12
MnO	0.26	0.26	0.16	0.27	0.076	0.01	0.01	0.038	0.059	0.23
P ₂ O ₅	0.2	0.24	ND	ND	ND	ND	ND	ND	ND	ND
Fe ₂ O ₃	14.13	13.5	5.08	6.46	1.42	1.2	0.68	0.15	0.2	0.3
Al ₂ O ₃	15.2	14	15.1	13.6	12	12.2	12.64	11.46	12.7	10
LOI	3.23	3.4	2	3	0.96	0.95	0.69	0.61	0.74	0.42
V	200.3	270	680	70.7	230	350	23.8	12.01	12	10.2
Cr	64.1	340.2	100.21	62	40.14	90.2	16.24	9	10	6
Cu	370	430	400	330.33	250	250	280	200	230.2	180
Sr	2160	2500	1400	2040	2940.12	2350.12	2160	1380.2	2510	750.46
Zr	2900.2	330.24	580.11	4300	750	760	320.34	250	210	170
Ba	1000	90.03	1000	3700	2400	989.7	500.02	1100	4400	<0.01
Zn	440	100.23	310.2	420	70.2	130.7	81.24	4.48	16	16.24
Ce	<0.01	<0.01	2	<0.01	2	0.8	1.56	1.5	<0.01	0.04
Pb	<0.01	75.7	370	<0.01	30	<0.01	180	100.22	100	16
Ga	<0.01	<0.01	1	0.1	1	1.2	1.6	1.3	0.9	0.5
As	<0.01	<0.01	<0.01	<0.01	0.2	<0.01	0.6	0.78	1.1	0.07
Y	<0.01	<0.01	<0.01	<0.01	<0.01	0.01	<0.01	0.06	0.87	0.8
Rb	190	150	<0.01	190	145	148	142	54	152	138
Nb	<0.01	<0.01	<0.01	<0.01	<0.01	<0.01	<0.01	<0.01	<0.01	<0.01
Hg	3	<0.01	<0.01	0.2	<0.01	<0.01	<0.01	<0.01	<0.01	<0.01
Ta	<0.01	<0.01	<0.01	<0.01	<0.01	<0.01	<0.01	<0.01	<0.01	<0.01
W	<0.01	<0.01	<0.01	<0.01	<0.01	<0.01	<0.01	<0.01	<0.01	<0.01
Hf	36	38.6	38.46	51.32	34.86	40.63	40.02	30.06	<0.01	24.6
Sn	<0.01	<0.01	1	<0.01	<0.01	<0.01	<0.01	<0.01	<0.01	<0.01
Sb	0.06	0.3	3.1	<0.01	<0.01	<0.01	<0.01	<0.01	<0.01	<0.01
Se	<0.01	<0.01	<0.01	<0.01	<0.01	<0.01	<0.01	<0.01	<0.01	<0.01
Bi	<0.01	<0.01	<0.01	<0.01	<0.01	<0.01	<0.01	<0.01	10.7	<0.01
Sc	<0.01	<0.01	<0.01	<0.01	<0.01	<0.01	<0.01	<0.01	<0.01	<0.01
Ni	<0.01	<0.01	<0.01	<0.01	<0.01	<0.01	<0.01	<0.01	<0.01	<0.01
Mo	0.18	<0.01	<0.01	0.2	<0.01	<0.01	<0.01	<0.01	<0.01	<0.01

Table 2: Cross, Iddings, Pirsson and Washington (CIPW) Table of the Rock groups

Samples	1	2	3	4	5	6	7	8	9	10
Orthoclase	5.910	2.837	0.000	3.428	7.092	7.683	7.092	22.457	23.639	5.718
Albite	2.541	1.694	0.000	3.642	3.642	3.557	6.776	10.418	8.809	8.639
Anorthite	13.742	16.759	7.616	13.320	7.936	7.440	2.976	3.026	4.166	2.678
Quartz	37.284	38.362	35.921	49.799	68.977	69.067	70.364	59.182	56.830	75.078
Magnetite	0.000	0.000	0.000	0.000	0.000	0.000	0.000	0.000	0.000	0.435
Hematite	14.130	13.500	5.080	6.460	1.200	1.420	0.680	0.150	0.200	0.000
Ilmenite	1.909	1.776	1.064	1.235	1.045	0.902	0.646	0.209	0.011	0.114
Biotite	13.889	6.963	1.840	7.791	2.484	2.885	1.272	1.341	0.329	0.305
Amphibole	10.678	19.209	42.419	10.092	0.000	0.000	0.000	0.000	0.000	0.000
Corundum	7.241	4.592	6.948	6.103	7.282	7.173	8.932	4.216	5.135	6.254
Sum	99.829	102.087	99.960	98.017	97.740	97.966	97.740	100.028	99.039	99.210

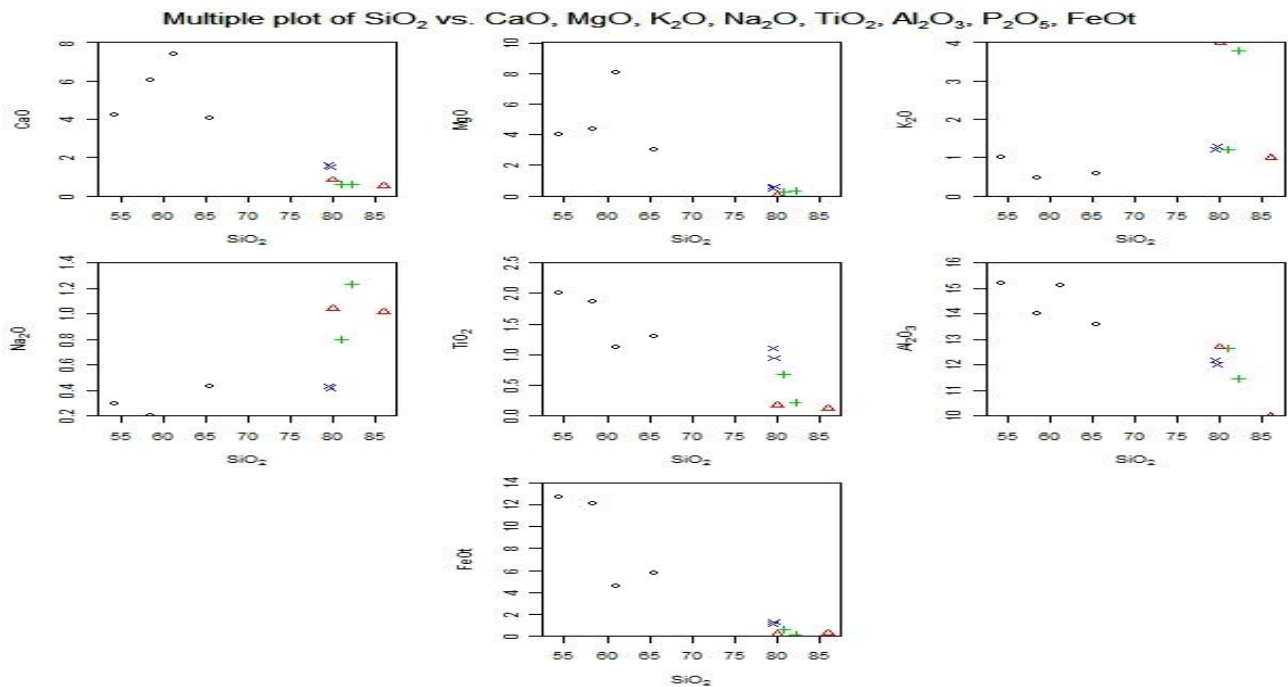


Figure 5: Harker diagrams for major elements of metatexites, melanocratic diatexites, mesocratic diatexites and leucocratic diatexites

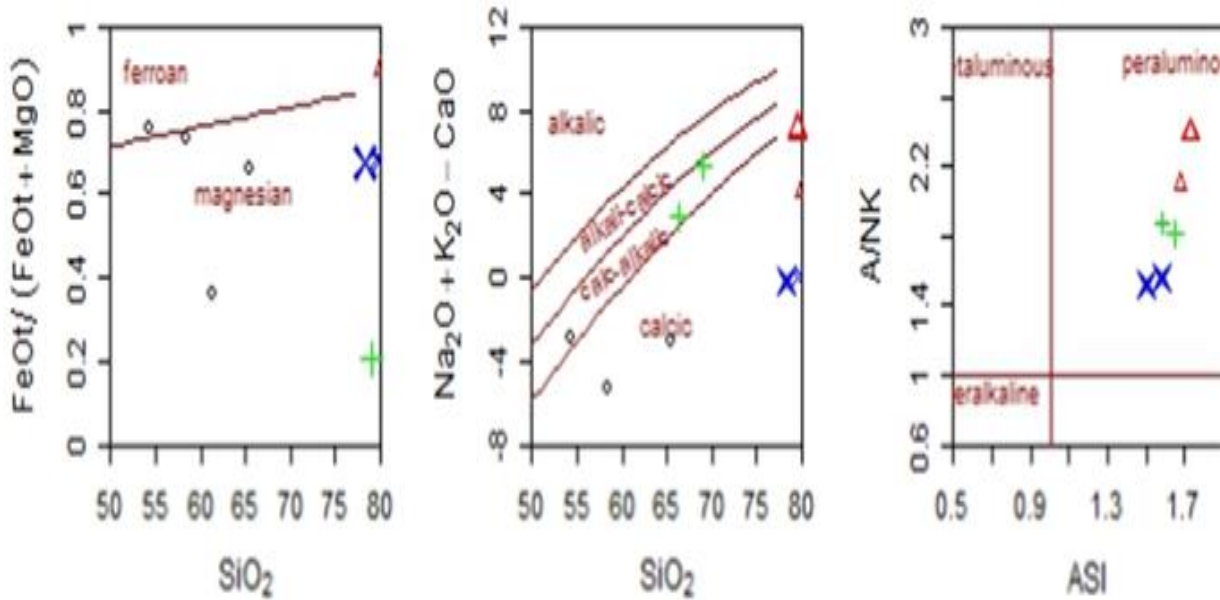


Figure 6: Granite tectonic discrimination diagram (after Frost 2001).

b) Tectonic Discrimination Diagram

The discrimination diagram of Frost et al. (2001) (figure 6) was employed, and on the modified alkali lime index (MALI), all the rock groups are plotted into ferroan and magnesian domains. Also, the metatext and melanocratic diatexites are plotted into the calcic field, whereas mesocratic and leucocratic diatexites show calc-alkalic to alkali-calcic characteristics. However, on the other hand, for the alumina saturation index (ASI), all the diatexites ranging from melanocratic diatexites to leucocratic diatexites are plotted into the peraluminous field.

c) Ternary Discrimination Diagram (AFM)

The three-component triangular graph (figure 7) shows the variation of mineral assemblages as a function of rock composition and includes tholeiitic and calc-alkaline magmatic differentiation trends. The metatexites/migmatite falls under sub alkaline series (they contain less sodium), whereas the melanocratic, mesocratic and leucocratic diatexites fall under the calc-alkaline series.

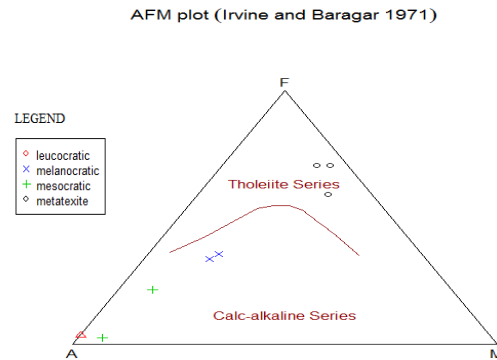


Figure 7: Ternary AFM discrimination diagram [after Irvine and Baragar (1971). A= (Na₂O+ K₂O), F= (Total Fe), M= (MgO) in percentage.]

d) Binary Discrimination Diagram (Silica Versus Potassium Oxide)

The metatexites are plotted into tholeiite to calc-alkaline series due to their ferromagnesian mineral contents. The melanocratic diatexites fall under the calc-alkaline series, whereas the mesocratic diatexites and leucocratic diatexites were plotted into the high-K calc-alkaline field due to the high potassic content of the rocks.

e) Feldspar Triangular Diagram (Mineral Chemistry)

Feldspar diagram shows a good correlation from anorthite depicting higher temperature for the metatexites to leucocratic diatexites with a fall in temperature (figure 9). The metatexites are plotted into anorthite field, and they are calcic rich, while leucocratic diatexites are plotted into an design field that is to say that they are fairly sodic rich. Melanocratic and mesocratic diatexites are in between the calcic and sodic ends.

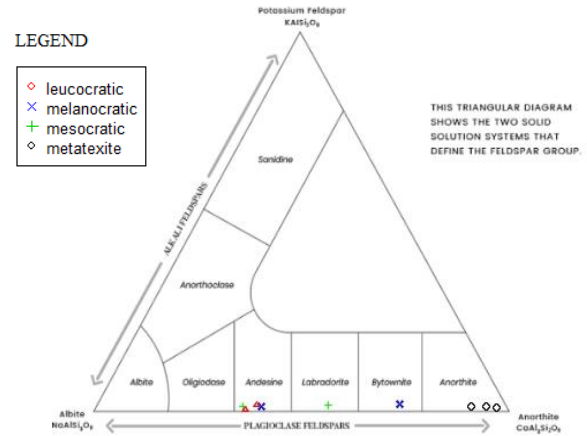


Figure 9: Feldspar triangular diagram

SiO₂-K₂O plot (Peccerillo and Taylor 1976)

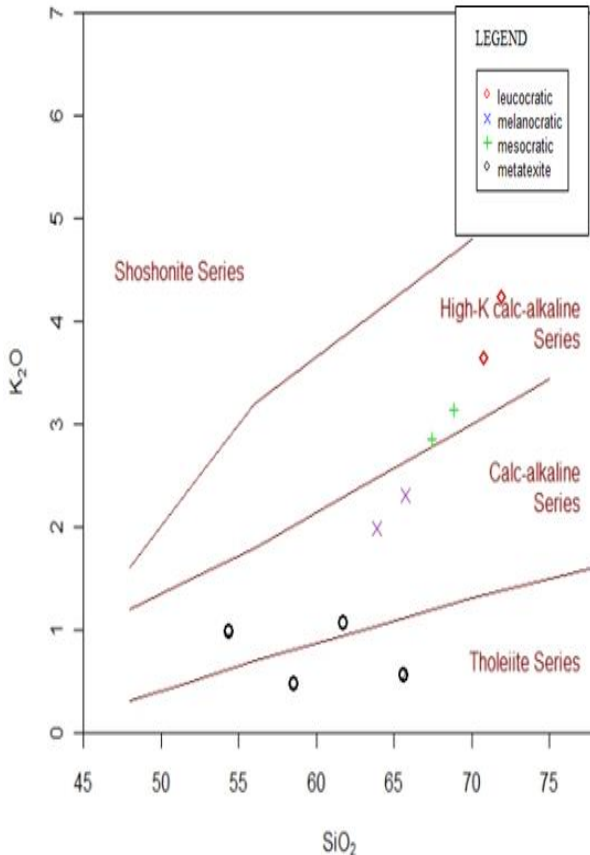


Figure 8: Discrimination binary diagram of K₂O against SiO₂ (after Peccerillo and Taylor 1979)

g) Spider plot

Multi-elemental variation diagram normalized to the composition of average upper crust after Sun et al. 1980 (figure 10) shows the variation of trace elements relative to compatibility and gives the behavioral patterns of the rock groups determined by the amount (quantity) of trace elements. The plot of metatexites shows enrichment in low iron lithophile elements (Rb, K & Sr) and depletion in high field strength elements (Ba, Nb & Y). On the other hand, the diatexites show relatively high field strength element contents (Se, Zr & Ba) and a higher low iron lithophile element content.

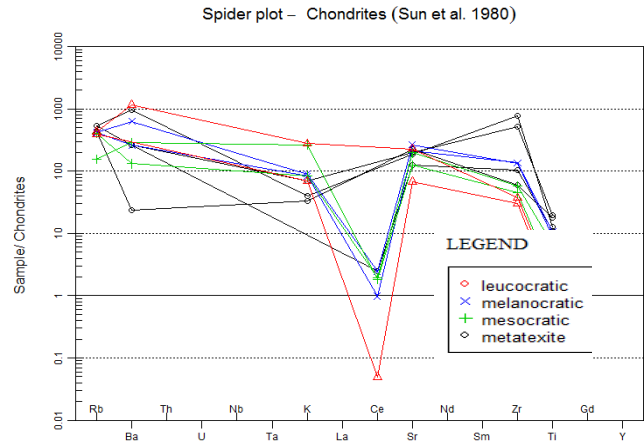


Figure 10: Spider diagram (after Sun et al. 1980)

V. Discussion

A. Morphological features

From the field relationship studies of the rocks of the study area, it can be deduced that the area consists of migmatites generated through different stages of partial melting. As partial melting occurs, compositional variation is expected to result from variable degrees of The melt-residuum separation between components and

fractional crystallization of the melt and subsequent development of different morphological forms.

Evidently, a realistic model put forward by (Renner et al. 2000) gives the transition between the different types of second-order morphologies of metatexite and diatexite migmatites on a scale of syn-anatectic strain versus melt fraction. For instance, the metatexite migmatite (figure 3A) has the neo some segregated into melanosome and leucosome and preserves its syn-anatectic structure that is primary layering. However, increased strain rate leads to disaggregation at relatively lower melt fractions as observed in the melanocratic diatexites of the study area (figure 3B). The difference in syn-anatectic strain tends to be an important factor with increase crystallization, and high shear strain generates better alignment of minerals schollen (raft) as seen in mesocratic diatexites (figure 3C), it has paleo some as raft leading to the development of compositional foliation.

B. Geochemical characteristics

Major oxides (wt.%) and minor/trace elements (ppm) data were used to generate the various geochemical plots, whereas CIPW and granite mesonorms were computed to ascertained index/accessory minerals. Both the metatexites and the diatexites show overlapping compositions, and the decreasing/ increasing trends on Harker diagrams (figure 5) indicate that both are petrogenetically related. However, most of the diatexites with (SiO₂ 79.7wt.% to 86.0wt.%) yield higher alkali feldspar, plagioclase feldspar, and quartz contents compared to the metatexites with (SiO₂ 54.3wt.% to 65wt.%), and here the leucocratic diatexites appeared to be the most fractionated of the diatexite types (O'Connor, 1965).

Again, from the plot of frost tectonic discrimination (figure 6), the rock groups occupy both the ferroan and magnesian fields, and relating it further to alumina saturation index plot (ASI), the peraluminous property of the diatexites implies high development of k-feldspar with continuous fractional crystallization as the system is cooling and temperature is dropping (Frost and Frost, 1997). Along with the work of (Chappell & white, 2001), the strongly peraluminous signature further suggests that there was crustal contamination during the anatexis event, and thus the occurrence of metasedimentary rocks within the study area strengthens the fact that there was a sedimentary input during the partial melting event.

On the ternary plot of (Irvine & Baragar 1971) (figure 7), the metatexites occupy the theoleiite series and therefore differ from the diatexites occupying the calc-alkaline series. As well plotted on feldspar triangular diagram (figure 9), metatexites fall under the calcic plagioclase, and on the petrographic studies of the rock groups, it is found to be coexisting with olivine and pyroxene (high-temperature minerals) through bytownite and labradorite for melanocratic

and mesocratic diatexites respectively with a farther migration towards sodic plagioclase for leucocratic diatexite portraying a decrease in temperature.

Spider plot (figure 10) normalized to the composition of average upper crust after (Sun et al. 1980) gives the behavioral trend of the rock groups. Partial melting of a mafic rock serves as a precursor to a parent magma (Matthias, 2006), the presence of patches of schist as a relic of palaeosome is true for the metatexite it can be deduced that the mesocratic diatexite was formed when metasedimentary rocks melted sufficiently to undergo bulk flow or magma flow but did not experience sufficient melt-residuum separation. Mostly, mesocratic diatexites that underwent melt segregation during flow generated a melanocratic diatexite at places where the melt fraction was removed, leaving behind a biotite and plagioclase residuum enriched in TiO₂, FeO, CaO, MgO, Cr, Ni, Sr, and a complementary leucocratic diatexites enriched in SiO₂, K₂O, and Rb where the melt fraction accumulated.

VI. Conclusion

The metatexites, melanocratic diatexites, mesocratic diatexites, and leucocratic diatexites are the rock types of the study area. Metasediments (schists and quartzites) are believed to be the parent rocks. Melt residuum separation at low degrees of partial melting and low melt fraction results in the formation of metatexites, whereas a high melt fraction and a nearly complete fusion of the melt forms the diatexite migmatites.

The rock groups portrayed geochemical continuity sequence of formation as a result of mineral differentiation trends of decreasing CaO, MgO, TiO₂, Al₂O₃, and FeO, with increasing SiO₂ from metatexites to leucocratic diatexites. Fractional crystallization is considered responsible for the evolution of the diatexites. High K₂O and Na₂O contents of the leucocratic diatexites show that they are the most evolved type of diatexites.

The behavioral trends of the rock groups and the variation of trace elements relative to compatibility show that the rock types are co-genetic and affected by the same geologic processes.

Acknowledgment

The completion of this undertaking could not have been possible without the participation and assistance of so many people whose names may not all be enumerated. Their contributions are sincerely appreciated and gratefully acknowledged.

However, I would like to express deep appreciation to my supervisor Prof. Ahmad Isah Haruna, and to my uncle, Alhaji Usman Magaji and Mallam Abdulmajid Isa Jibrin am equally grateful.

To my parents, siblings and friends, and others who, in one way or another, shared their support, either morally, financially, and physically, thank you all.

References

- [1] Black, R. and Liegeois, J. P., Cratons, mobile belts, alkaline rocks, and continental lithospheric mantle: The Pan-African testimony. *Journal of the Geological Society, London*, **150** (1993) 89-98
- [2] Chappell BW, White A.J.R., Two Constrating Granite Types. 25 Years Later. *Australian .*, (2001). *Journal of Earth Sciences*, 48 (1998) 489-499
- [3] Ferre, E.C., Caby, R., Peucatt, J.J., Capdevila, R., & Monie, P., Pan-African post-Collisional ferro-potassic granite and quartz-monzonite plutons of Eastern Nigeria. *Lithos*, 45 255-278.
- [4] Ferre, E. C., Gleizes. G., and Caby, R., Tectonics and post-collisional granite Emplacement in an obliquely convergent orogen: the Trans-Saharan belt, Eastern Nigeria. *Precambrian Research*, 114(2002) 199-219.
- [5] Ferre, E.C., and Caby, F., GranuliteFacies Metamorphism & Charnockitic Plutonism: Examples from the Neoproterozoic Belt of Northern Nigeria. *Proceedings of the Geologists' Association*, 118 (2006)1-8
- [6] Frost B.R, and Barnes C.G. *Journal of petrology* 42(11) (2001) 2033-2048.
- [7] Frost CD, Frost BR. High-K, iron-enriched Rapakivi-type granites: the tholeiite connection. *Geology* (1997) 25:647–50.
- [8] Matthias Forwick.; West, Gabriel; Kaufman, Darrell S; Muschitiello, Francesco; Matthiessen, Jens; Wollenburg, Jutta; O'Regan, Matt. Amino acid racemization in Quaternary foraminifera from the Yermak Plateau, Arctic Ocean. *Quaternary Geochronology* 2019; ISSN 1871-1014.s , 1(2019) 53 - 67.s doi: 10.5194/gchron-1-53-2019.
- [9] O'Connor, J. T., A classification of quartz-rich igneous rock-based on feldspar ratio. *United States Geological Survey Paper* 525-B,(1965) 79-89.
- [10] Oyayoye M.O. On the occurrence of Fayalite Quartz- Monzonite in the basement complex around Bauchi, Northern Nigeria. *Geol.*, 70(5) (1962) 473-82.
- [11] Peccerillo, A. and Taylor, S.R., Geochemistry of Eocene Calc-Alkaline Volcanic Rocks from the Kastamonu area, Northern Turkey., (1979).
- [12] Renner J, Evans B, and Hirth G., On the rheologically critical melt fraction. *Earth and Planetary Science Letters* (2000) 191:585–594.
- [13] Sawyer, E.W., Criteria for the recognition of partial melting. *Phys. Chem. Earth (A)* 24 (1998) 269-279
- [14] Sawyer EW., Atlas of Migmatites. *Canadian Mineralogist Special Publication* 9, NRC Research Press, Ottawa, Ontario, Canada., (2008a).
- [15] Sun S.S. *Philosophical Transactions of the Royal Society of London. Series A, Mathematical and Physical Sciences* 297 (1431) (1980) 409-445.